Molecular Plant Pathology

MOLECULAR PLANT PATHOLOGY (2018) **19**(10), 2263–2276 DOI: 10.1111/mpp.12697

The plant-parasitic cyst nematode effector GLAND4 is a DNA-binding protein

STACEY N. BARNES[1], CATHERINE L. WRAM[1,†], MELISSA G. MITCHUM[2] AND THOMAS J. BAUM [1,*]

[1]*Plant Pathology & Microbiology Department, Iowa State University, Ames, IA 50011, USA*

[2]*Division of Plant Sciences and Bond Life Sciences Center, University of Missouri, Columbia, MO 65211, USA*

SUMMARY

Cyst nematodes are plant pathogens that infect a wide range of economically important crops. One parasitic mechanism employed by cyst nematodes is the production and *in planta* delivery of effector proteins to modify plant cells and suppress defences to favour parasitism. This study focuses on GLAND4, an effector of *Heterodera glycines* and *H. schachtii*, the soybean and sugar beet cyst nematodes, respectively. We show that GLAND4 is recognized by the plant cellular machinery and is transported to the plant nucleus, an organelle for which little is known about plant nematode effector functions. We show that GLAND4 has DNA-binding ability and represses reporter gene expression in a plant transcriptional assay. One DNA fragment that binds to GLAND4 is localized in an *Arabidopsis* chromosomal region associated with the promoters of two lipid transfer protein genes (*LTP*). These LTPs have known defence functions and are down-regulated in the nematode feeding site. When expressed in Arabidopsis, the presence of GLAND4 causes the down-regulation of the two *LTP* genes in question, which is also associated with increased susceptibility to the plant-pathogenic bacterium *Pseudomonas syringae*. Furthermore, overexpression of one of the *LTP* genes reduces plant susceptibility to *H. schachtii* and *P. syringae*, confirming that *LTP* repression probably suppresses plant defences. This study makes GLAND4 one of a small subset of characterized plant nematode nuclear effectors and identifies GLAND4 as the first DNA-binding, plant-parasitic nematode effector.

Key words: DNA-binding effector, GLAND4, host–parasite interaction, *LTP*, soybean cyst nematode

INTRODUCTION

Cyst nematodes are sedentary root endoparasites that infect a wide range of economically important crops, including soybean. The soybean cyst nematode, *Het erodera glycines*, is the number one pathogen of soybean, causing over $1 billion in annual yield losses in the USA (Allen *et al.*, 2017; Koenning and Wrather, 2010). Successful cyst nematode infection involves the avoidance or suppression of host defences, whilst penetrating into the roots of host plants and establishing a feeding site close to the plant vasculature (Endo, 1964). The initial feeding cell is expanded through dissolution of the surrounding cell walls to form a multinucleated structure, referred to as a syncytium (Jones, 1981; Jones and Northcote, 1972). Gene expression profiling studies performed on whole roots and microdissected syncytia have revealed extensive alterations in host gene expression in response to cyst nematode infection (Hermsmeier *et al.*, 1998; Hofmann *et al.*, 2010; Ithal *et al.*, 2007; Puthoff *et al.*, 2003; Szakasits *et al.*, 2009; Wan *et al.*, 2015). The secretion of effector proteins, defined by their ability to modify host cell structure and function, is key to the breakdown of plant tissue for migration and the suppression of plant defences (Hewezi *et al.*, 2010; Hogenhout *et al.*, 2009; Wang *et al.*, 1999). Effectors also play a prominent role in the induction of host cell morphological and physiological changes required for syncytium formation and maintenance (Hewezi and Baum, 2013; Mitchum *et al.*, 2013). Therefore, effectors, directly or indirectly, are responsible for many of the gene expression changes observed in the host plant. However, the molecular mechanisms for the triggering of gene expression changes remain mostly elusive. The majority of known plant nematode effectors are synthesized in three specialized secretory cells, a single dorsal and two subventral glands, before being secreted through a mouthspear known as the stylet (Hussey, 1989; Vieira *et al.*, 2011). Once inside the plant tissue, effectors have been shown to accumulate in the apoplast (Hewezi *et al.*, 2008; Lozano-Torres *et al.*, 2012; Vieira *et al.*, 2011; Wang *et al.*, 2010), as well as in various compartments within the plant cell, including the nucleus (Elling *et al.*, 2007; Hewezi *et al.*, 2015; Jaouannet *et al.*, 2012; Jones *et al.*, 2009; Postma *et al.*, 2012; Zhang *et al.*, 2015), where little is currently known about effector functionality.

More than 80 candidate effectors have been identified through isolation and sequencing of RNA within the gland cells of *H. glycines* (Gao *et al.*, 2001, 2003; Noon *et al.*, 2015; Wang *et al.*, 2001). The sequences have been subjected to bioinformatic filtering

*Correspondence: Email: tbaum@iastate.edu

†*Present address:* Department of Botany & Plant Pathology, Oregon State University, Corvallis, OR 97330, USA

and verification of transcript accumulation in the gland cells to ensure a high likelihood of secretion during parasitism (Noon *et al.*, 2015). The characterization of a subset of these candidate effectors by the identification of effector–plant protein interactions has revealed functions relating to cell wall modification, antioxidant production, hormone signalling, plant defence suppression and host peptide mimicry (Hamamouch *et al.*, 2012; Hewezi *et al.*, 2008, 2010, 2015; Lee *et al.*, 2011; Noon *et al.*, 2016; Patel *et al.*, 2010; Pogorelko *et al.*, 2016; Vanholme *et al.*, 2009; Wang *et al.*, 2005). Effectors in other pathogens, most notably *Xanthomonas* spp., are known to interact directly with host DNA to modify host gene transcription (de Lange *et al.*, 2013; Li *et al.*, 2013; Nissan *et al.*, 2006; Padavannil *et al.*, 2014; Yang *et al.*, 2000). Transcription activator-like effectors (TALEs) in *Xanthomas* spp. can bind directly to the promoter of host genes, resulting in increased transcription triggered by an activation domain found at the C-termini of the effectors. Altered host expression can result in increased virulence or avirulence depending on the host and bacterial strain (Bing and White, 2004; Kay *et al.*, 2007; Sugio *et al.*, 2007; Szurek *et al.*, 2001). The *Meloidogyne incognita* effector 7H08 represents the first documented case of transcriptional activation in plant-pathogenic nematodes, but the target genes and mechanism of activation have yet to be elucidated (Zhang *et al.*, 2015). Despite the massive plant gene expression changes accompanying nematode infections, there are currently no peer-reviewed published records of DNA-binding effectors in plant-parasitic nematodes. This is a result, in part, of a sparse understanding of plant nuclear-targeted nematode effectors. Plant-pathogenic, DNA-binding effectors are not limited to gene activation, as the *Xanthomonas* effector XopD binds non-specifically to DNA and actually represses the transcription of reporter genes (Kim *et al.*, 2008). The identification of a transcriptionally repressing effector and its *in vivo* targets would represent a breakthrough discovery in the study of molecular plant–pathogen interactions.

This study details the functional characterization of GLAND4 as the first DNA-binding, plant-parasitic nematode effector. GLAND4 is a dorsal gland-produced cyst nematode effector that is recognized and transported to the host nucleus. Sequence analysis suggests that GLAND4 is a potential DNA-binding effector because of similarities with histone-like proteins and known transcriptional activators. GLAND4 homologues from *H. glycines* and the sugar beet cyst nematode *H. schachtii* share 95% amino acid identity. Functional characterization of GLAND4 has been conducted using *H. schachtii*, which can successfully parasitize the model plant *Arabidopsis thaliana* (Sijmons *et al.*, 1991). This report shows that GLAND4 is a DNA-binding effector with the ability to repress gene expression when located in close proximity to the transcriptional start site (TSS) of a reporter gene. Two host genes located within an identified GLAND4-binding region are two *A. thaliana* lipid transfer proteins (LTPs), which belong to a multigene family involved in a variety of processes, including resistance to biotic and abiotic stressors (Ambrose *et al.*, 2013; Jung *et al.*, 2003; Liu *et al.*, 2015). *LTP* overexpression is known to increase pathogen resistance; therefore, the down-regulation of such genes by GLAND4 would be advantageous for host infection (Jung *et al.*, 2005).

RESULTS

Sequence analysis and transcript localization of GLAND4 *orthologues*

The candidate effector *GLAND4* was initially discovered after performing microaspiration and sequencing of *H. glycines* oesophageal gland cell RNA (Noon *et al.*, 2015). To gain an insight into whether GLAND4 is a feasible candidate for functional analysis in the model plant *A. thaliana*, the *GLAND4* sequence was identified in *H. schachtii* cDNA. Unlike *H. glycines*, *H. schachtii* successfully infects *A. thaliana*, allowing for more in-depth functional analyses (Gheysen and Fenoll, 2011; Sijmons *et al.*, 1991). A pairwise sequence alignment of the GLAND4 predicted proteins from *H. glycines* and *H. schachtii* displayed a 95% identity, indicating that GLAND4 is a good candidate for functional characterization using *A. thaliana* (Fig. S1, see Supporting Information). Therefore, all subsequent analyses have utilized *H. schachtii* GLAND4 unless otherwise stated.

As most known nematode effectors are synthesized within the specialized secretory gland cells of the nematode, the localization of *GLAND4* transcripts within *H. schachtii* was assessed by *in situ* hybridization using a labelled probe complementary to *GLAND4*. A strong signal resulting from successful probe hybridization was detected in the dorsal gland of *H. schachtii*, revealing an accumulation of *GLAND4* transcripts within this cell type (Fig. 1A). The dorsal gland localization of *GLAND4* is consistent with previous findings in *H. glycines* (Noon *et al.*, 2015).

GLAND4 has a 543-nucleotide open reading frame, translating to a predicted protein length of 180 amino acids, which contains an N-terminal signal peptide. The signal peptide is cleaved as part of the protein trafficking process within the nematode and is therefore not included in any subsequent GLAND4 analyses, which is denoted by '*-SP*' in the gene construct names. Not counting the signal peptide, GLAND4 exhibits a high percentage of lysine residues at the N-terminus: 36 of the first 86 residues (42%) are lysines, suggesting that GLAND4 may form electrostatic interactions with the negatively charged DNA backbone. The lysine-rich region is followed by a charge-neutral linker region and an acidic C-terminal region (Fig. S1). The positioning of acidic and hydrophobic amino acids in the C-terminal domain bares resemblance to that found in TALEs and other proteins possessing an acidic activation domain (Table S1, see Supporting Information).

GLAND4 contains three overlapping predicted bipartite nuclear localization signals ranging from amino acids 37 to 61,

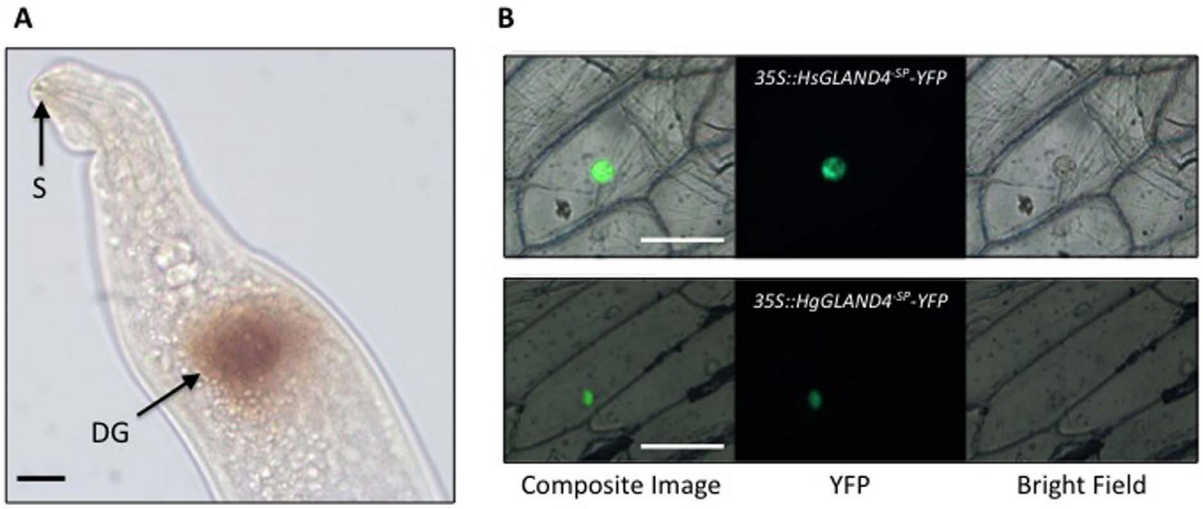

Fig. 1 Localization of GLAND4. (A) *In situ* hybridization showed a localization of *GLAND4* within the dorsal gland of *Heterodera schachtii* on hybridization to an antisense digoxigenin-labelled DNA probe. DG, dorsal gland cell; S, stylet. Scale bar, 10 μm. (B) Subcellular localization revealed that *35S::HsGLAND4^{-SP}-YFP* (top panels) and *35S::HgGLAND4^{-SP}-YFP* (bottom panels) were targeted to the nucleus of plant cells when expressed in onion epidermal cells using particle bombardment. YFP, yellow fluorescent protein. Scale bar, 200 μm. Results shown in (A) and (B) are representative of three independent experiments, each with at least 10 biological replicates.

and GLAND4 is predicted to accumulate within the plant nucleus (PSORTII) (Fig. S1). To test this prediction *in planta*, the *GLAND4H. schachtii* and *H. glycines* coding sequences were placed under the control of the cauliflower mosaic virus (CaMV) 35S promoter and fused to the yellow fluorescent protein (YFP) coding sequence to create *35S::HsGLAND4^{-SP}-YFP* and *35S::HgGLAND4^{-SP}-YFP*. The fusion protein constructs were bombarded into onion epidermal cells in which green fluorescent protein (GFP) signals were localized exclusively in the plant nucleus (Fig. 1B).

To gain an insight into the potential role of GLAND4, a BLASTP search was performed against the National Center for Biotechnology Information (NCBI) non-redundant database. Apart from hits to *Het erodera* and *Globodera*, which is another CN genus, the N-terminal region of GLAND4, amino acids 36–55, contained a repeat region with similarity to histone proteins from a variety of organisms (Table S2, see Supporting Information). The distribution of charges, homology to known transcription factors and nuclear localization *in planta* suggested that GLAND4 has the potential to function as a DNA-binding transcription factor-like protein.

GLAND4 increases pathogen susceptibility in A. thaliana

To determine the role of GLAND4 during infection, three independent homozygous *A. thaliana* T3 lines (3-10, 5-6 and 6-1), constitutively expressing the *GLAND4* coding sequence, were developed to test alterations in pathogen susceptibility. *GLAND4* expression was verified using quantitative reverse transcription-polymerase chain reaction (qRT-PCR) (Fig. S2, see Supporting Information). None of the transgenic lines displayed phenotypic differences or differences in susceptibility to *H. schachtii* relative to wild-type Columbia-0 (Col-0) (Fig. S3, see Supporting Information). The fact that *H. schachtii* is already delivering GLAND4 into host plants may account for the observation that the additional GLAND4 production in lines 3-10, 5-6 and 6-1 did not increase susceptibility. However, in order to assess the broader role of GLAND4 in defence suppression, the same *GLAND4*-expressing *A. thaliana* lines were infected with the bacterial plant pathogen *Pseudomonas syringae* pv. *tomato* (*Pst* DC3000), which does not use a GLAND4 effector as part of its normal plant infection. Transgenic lines 5-6 and 6-1 displayed an increase in susceptibility relative to Col-0, demonstrating that *GLAND4* is able to influence plant susceptibility to pathogens (Fig. 2).

GLAND4 is a DNA-binding protein

Based on the similarity of GLAND4 to histone proteins, genomic Systematic Evolution of Ligands by EXponential enrichment (SELEX) analysis (Shostak *et al*., 2004) was performed to detect possible DNA-binding properties of GLAND4. Genomic SELEX allows for the isolation of DNA sequences with a high affinity for GLAND4 through multiple rounds of binding of the DNA fragments to GLAND4, followed by subsequent PCR amplification and sequencing. The procedure was carried out using recombinant FLAG-GLAND4-HIS protein and enzymatically digested

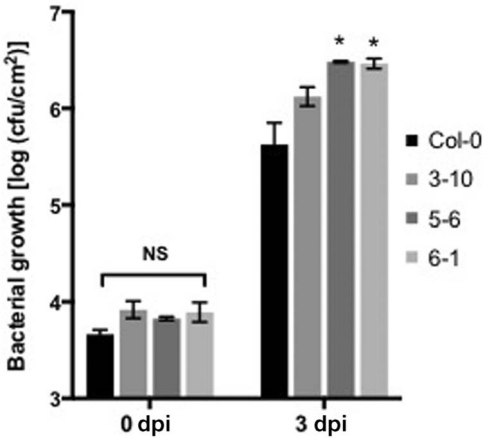

Fig. 2 GLAND4 increases susceptibility to *Pseudomonas syringae*. Bacterial titres (cfu, colony-forming units) of independent homozygous *Arabidopsis thaliana* T3 lines (3-10, 5-6 and 6-1) constitutively expressing *GLAND4*$^{-SP}$. *Arabidopsis thaliana* leaves were measured at 2h [0 days post-inoculation (dpi)] and 72h (3 dpi) after syringe infiltration with *Pseudomonas syringae* pv. *tomato* (*Pst* DC3000). Differences in bacterial counts were determined in two independent experiments, each using four biological and three technical replicates. Bars represent the log transformation of averages from one of two independent experiments. A *t*-test was used to determine differences between the transgenic susceptibility relative to Col-0 *A. thaliana*. NS, not significant. ±SE (standard error), $^*P < 0.05$.

Col-0 genomic DNA. Four rounds of purification and enrichment were performed (Fig. 3A). Aliquots of the eluted DNA from rounds 2, 3 and 4 were cloned and transformed into *Escherichia coli*, and a total of 170 bacterial colonies were sequenced, yielding 59 unique DNA fragments (Fig. 3B). The fragments ranged between 333 and 985 bp in length, with an average length of 655 bp. Of the 20 unique fragments identified after round 4, 11 were derived from the *A. thaliana* nuclear genome, with the remaining fragments aligning to chloroplast and mitochondrial DNA. In an effort to test the hypothesis that GLAND4 functions as a DNA-binding transcription factor, attention was focused on two fragments which mapped to nuclear regions that were less than 3 kB from a TSS, subsequently referred to as GLAND4 responsive elements (G4RE1 and G4RE2). Another noteworthy finding was a fragment from SELEX round 3 that corresponded to the coding region of growth regulating factor 7 (GRF7). This discovery was also scrutinized further because other members of this transcription factor group (GRF1 and GRF3) have been shown previously to be key factors in cell reprogramming during *H. schachtii* infection (Hewezi *et al*., 2012).

Binding of the G4RE1, G4RE2 and GRF7 fragments to GLAND4 was confirmed using an electrophoretic mobility shift assay (EMSA) (Fig. 3C). Lanes containing GLAND4 showed a shifted band as a result of a decreased mobility of labelled DNA, which is indicative of the formation of protein–DNA complexes (Fig. 3C). To ensure that the shifted bands indicating protein–DNA binding were specific to GLAND4, reactions using the same DNA fragments, G4RE1, G4RE2 and GRF7, were performed using the unrelated cytoplasmically located *H. schachtii* effector 28B03 in place of GLAND4. Lanes containing 28B03 did not display a shift in DNA, indicating that binding only occurs in the presence of GLAND4 (Fig. 3C). As all three tested fragments showed some level of decreased mobility in the presence of GLAND4, a control DNA fragment was generated from a sequence located within a 1.5-kB region of G4RE2. No binding was observed for the control fragment in the presence of GLAND4 (Fig. 3D, right panel, lane 2).

The variation in intensity of the shifted bands for lanes containing GLAND4 suggests a stronger affinity for G4RE2 than for G4RE1 and GRF7, making G4RE2 the focus of further investigation (Fig. 3C). To further quantify such suspected affinity differences, a competitor EMSA was performed with the strongest shifted band (G4RE2) and the weakest shifted band (GRF7). An abundance of unlabelled G4RE2 or GRF7 was used as a competitor probe in reactions that all contained a uniform amount of labelled G4RE2. The HsGLAND4–G4RE2 complex was more strongly affected in the presence of G4RE2 competitor (Fig. 3D, left panel, lanes 3 and 4) than in the presence of GRF7 (Fig. 3D, left panel, lane 5), indicating that GLAND4 binds more strongly to G4RE2 than to GRF7.

Repression of genes in the region of G4RE2

G4RE2 is a 122-bp fragment that maps in the untranslated region (UTR) of *AT3G22600* (NM_113159), approximately 50 nucleotides downstream of the TSS. G4RE2 is also located less than 1 kB upstream of the TSS of *AT3G22620* (NM_113160) (Fig. 4A). The two genes associated with G4RE2 are part of a large family of LTPs, some of which are known to have altered gene expression in response to pathogen infection (Consales *et al*., 2012; Larroque *et al*., 2013; Molina and Garcia-Olmedo, 1993; Qutob *et al*., 2006). The proximity and orientation of the two *LTP*s in relation to G4RE2 suggests that the expression of both genes could be affected by the binding of GLAND4 to G4RE2. To test this hypothesis, *LTP* expression was measured in 3-week-old *GLAND4*-transgenic *A. thaliana* seedlings from the T3 lines 3-10, 5-6 and 6-1 (Figs 4B and S4, see Supporting Information). The expression level of *AT3G22630* was also quantified as a control gene because of its downstream location and opposite orientation, in relation to G4RE2, which suggests that *AT3G22630* is unlikely to be affected by the presence of GLAND4 (Fig. 4A). qRT-PCR showed at least a two-fold decrease in the mRNA abundance of *AT3G22600* and *AT3G22620* in *GLAND4* expression lines when compared with Col-0 (Fig. 4B). The down-regulation of both *LTP* genes observed in this study is supported by previous findings, which showed the

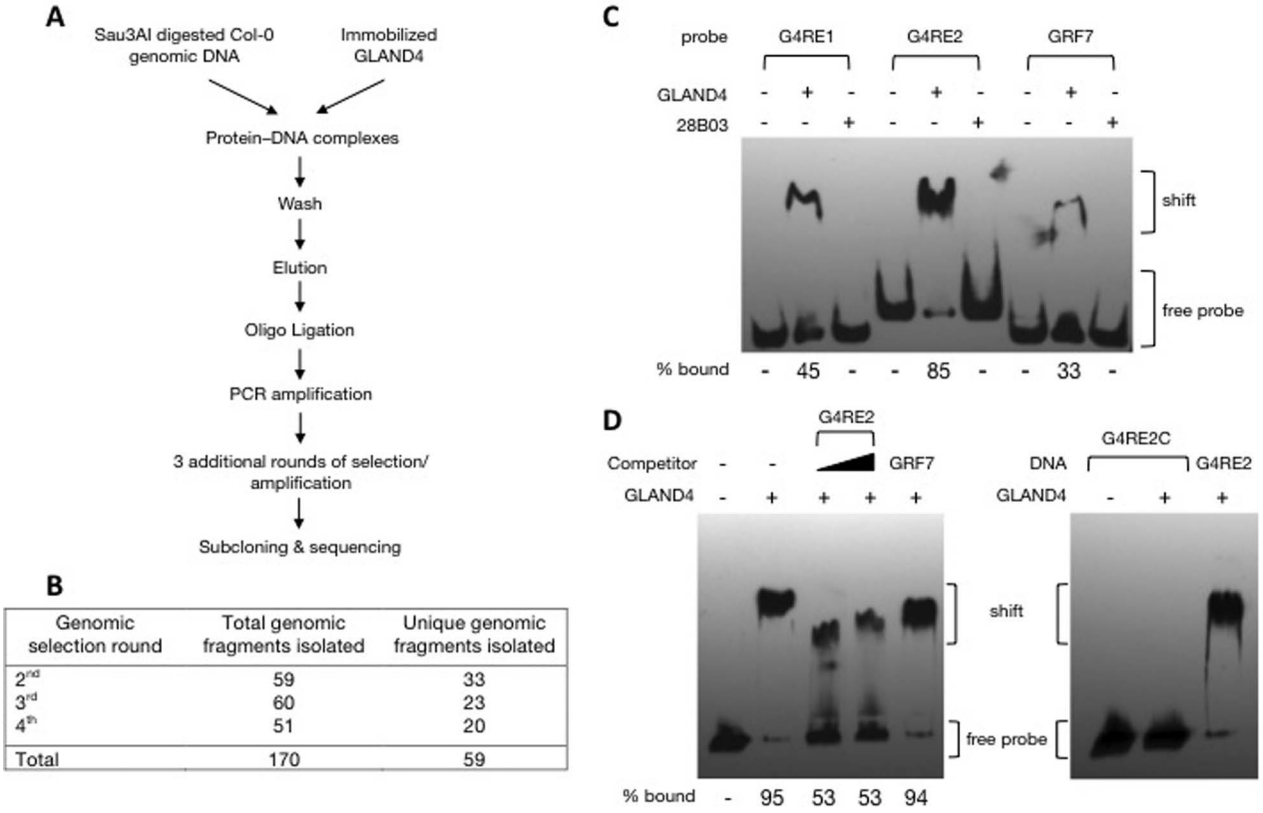

B

Genomic selection round	Total genomic fragments isolated	Unique genomic fragments isolated
2nd	59	33
3rd	60	23
4th	51	20
Total	170	59

Fig. 3 Characterization of GLAND4 DNA binding and confirmation of G4RE2 specificity. (A) Flow chart of the method for *in vitro* genomic selection. PCR, polymerase chain reaction. (B) Summary of the sequencing results for the *in vitro* genomic selection with GLAND4^{-SP}. (C) An electrophoretic mobility shift assay (EMSA) with biotin-labelled DNA probes for three selected fragments (G4RE1, G4RE2 and GRF7). The DNA was incubated without any effector protein, with recombinant GLAND4^{-SP} or with recombinant 28B03^{-SP}, a cytoplasmically localized effector. (D) Left: a competitive binding EMSA using biotin-labelled G4RE2. GLAND4^{-SP} was incubated with 200- and 500-fold molar excess of G4RE2 (lanes 3 and 4) or with 200-fold GRF7 (lane 5) unlabelled DNA. Right: an EMSA using a biotin-labelled control DNA fragment (G4RE2C), which is located <1.5 kB downstream from G4RE2. The results shown are representative of two independent experiments.

down-regulation of both genes within the microaspirated contents of the *H. schachtii* feeding site (Szakasits *et al*., 2009). However, the expression level of *AT3G22630* was unaffected in the *GLAND4* lines (Fig. 4B).

GLAND4 represses the expression of a reporter gene *in planta*

An *in planta* transient expression system involving the *GFP* reporter gene was utilized to investigate the transcriptional repression capabilities of GLAND4. In order to engineer changes in *GFP* expression, the bacterial LexA-responsive element *2xLexAop* and the yeast-responsive element *6xGAL4UAS* were incorporated upstream of the *GFP* start codon (Fig. 5A).

Incorporation of *2xLexAop* and *6xGAL4UAS* into the promoter region of *GFP* allows for the binding and manipulation of *GFP* expression using the LexA and GAL4 DNA-binding domain (GAL4BD). The ability of proteins to regulate *GFP* expression can then be tested through the fusion of experimental coding sequences to either *LexA* or *GAL4BD* to generate *35S::LexA-regulator* or *35S::GAL4BD-regulator* (Fig. 5A). The basal level of *GFP* mRNA was established after co-infiltration of the reporter with both binding elements in the absence of experimental coding sequences (Fig. 5B). In order to confirm GLAND4 as a transcriptional repressor, high levels of *GFP* were then induced using the transactivational domain *VP16* from herpes simplex virus fused to *GAL4BD*. As anticipated, the co-infiltration of *35S::GAL4BD-VP16* and *35S::LexA* alone resulted in an increase in *GFP* mRNA (Fig. 5B). To test the role of GLAND4 as a transcriptional repressor, the reporter was co-infiltrated with *35S::GAL4BD-VP16* and *35S::LexA-GLAND4*. Consistent with the hypothesis that GLAND4 functions as a repressor, the presence of GLAND4 yielded a significant reduction in *GFP* mRNA (Fig. 5B). To

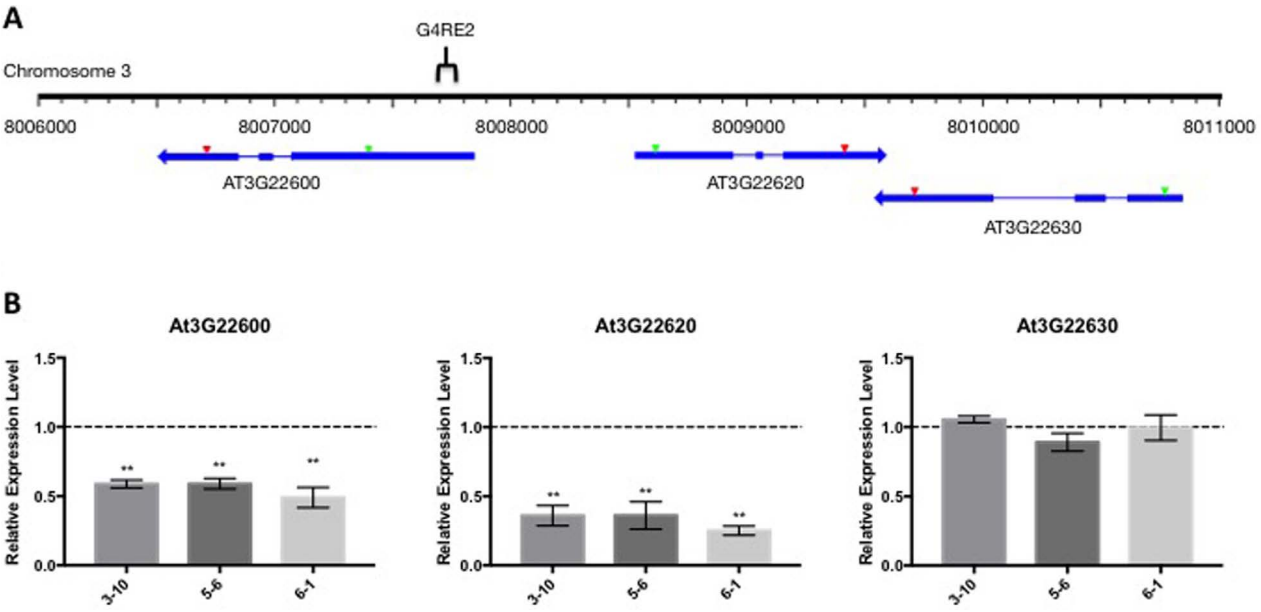

Fig. 4 Genes in the region of G4RE2 are down-regulated in GLAND4-transgenic *Arabidopsis thaliana*. (A) Arrangement of the genomic region surrounding G4RE2. Green and red arrowheads indicate the start and stop codons, respectively. (B) Expression of the two genes (AT3G22600 and AT3G22620) closest to G4RE2 and the next-nearest gene (AT3G22630) was measured in 3-week-old transgenic *A. thaliana* expressing *GLAND4*^{SP} using quantitative polymerase chain reaction (qPCR). Data were normalized to *Actin8* as an internal control and consist of two independent experiments, each with three biological replicates and four technical replicates. A *t*-test was used to identify means that were significantly different from Col-0 *A. thaliana*, set at 1.0, represented by a broken line. Bars represent the averages ± standard error (SE); $^{**}P < 0.0001$.

ensure that the *GFP* mRNA reduction was observed specifically in the presence of GLAND4, and not just as a by-product of any protein fused to LexA, a comparably sized portion of the *β-glucuronidase* (*GUS*) coding sequence was fused to *LexA* as a negative control. As anticipated, co-infiltration of the *35S::LexA-GUS* fusion with *35S::GAL4BD-VP16* displayed similar levels of *GFP* expression to that of the co-infiltration of *35S::LexA* with *35S::GAL4BD-VP16* (Fig. 5B). Therefore, the specific reduction of *GFP* mRNA levels in the presence of GLAND4 is consistent with the hypothesis that GLAND4 functions as a transcriptional repressor.

LTP down-regulation occurs during *H. schachtii* infection

To verify that *AT3G22600* and *AT3G22620* down-regulation is a bone fide strategy during cyst nematode infection, qRT-PCR was performed on *H. schachtii*-inoculated and non-inoculated Col-0 root tissue. The root tissue was harvested at 4, 7 and 14 days post-inoculation (dpi) to represent the gene expression changes incurred through the early infection period. *AT3G22600* showed a two- to four-fold down-regulation across all time points in *H. schachtii*-inoculated tissue relative to mock-inoculated tissue (Fig. 6A, B). *AT3G22620* showed a two-fold and 1.5-fold reduction at 7 and 14 dpi, respectively (Fig. 6A, B). Analysis of *GLAND4* mRNA abundance in the inoculated root tissue revealed that *GLAND4* expression peaks at the time point corresponding to the lowest level of expression for both *LTP*s (Fig. 6). This correlation of expression shows support for the role of GLAND4 in the down-regulation of *LTP*s.

Overexpression of *LTP*s decreases pathogen susceptibility in *A. thaliana*

In an effort to counteract *LTP* down-regulation and to explore the importance of LTPs during *H. schachtii* infection, both *LTP* genes (*AT3G22600* and *AT3G22620*) were individually expressed in *A. thaliana* under the control of CaMV 35S (Fig. S4A, B), which does not contain a known GLAND4-responsive element. The stable transgenic lines were challenged separately with *H. schachtii* and *Pst* DC3000. Two of the three *AT3G22600*-overexpressing transgenic lines demonstrated a reduction in *H. schachtii* susceptibility (Fig. 7A) and all transgenic lines for both *LTP*s demonstrated a decrease in susceptibility to *Pst* DC3000 (Fig. 7B).

DISCUSSION

This study analysed the functional role of the dorsal gland effector GLAND4 of *Heterodera* cyst nematodes. High similarity between

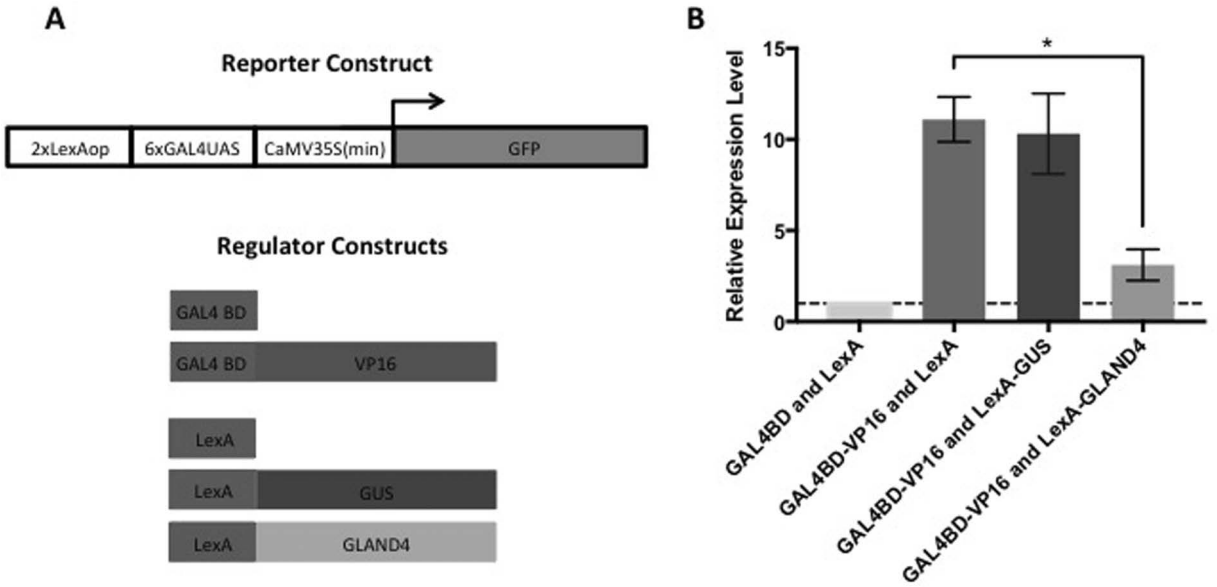

Fig. 5 GLAND4 represses reporter gene expression *in planta*. (A) A schematic representation of the reporter and regulator constructs used in the assay. The bacterial promoter LexAop was fused to the 6xGAL4UAS yeast promoter and inserted upstream of *GFP* in a binary T-vector to create a reporter construct. Regulator constructs were created by fusing the coding sequences of experimental proteins to either LexA or GAL4BD to initiate binding of experimental proteins to the promoter region of the *GFP* reporter gene. All regulator constructs were driven by the cauliflower mosaic virus (CaMV) 35S promoter. (B) *GFP* expression was quantified by quantitative reverse transcription-polymerase chain reaction (qRT-PCR) in the presence of varying combinations of GAL4BD and LexA regulator fusion constructs. Data were normalized to the expression of *hygromycin* and consist of two independent experiments, each with three biological replicates and four technical replicates. Expression levels were calculated relative to the level of *GFP* co-infiltrated with GAL4BD and LexA, which was set at 1.0, represented as a broken line. A *t*-test was used to identify means that were significantly different from VP16-activated green fluorescent protein (GFP) and LexA without a fusion protein. Bars represent the averages ± standard error (SE); $*P < 0.01$.

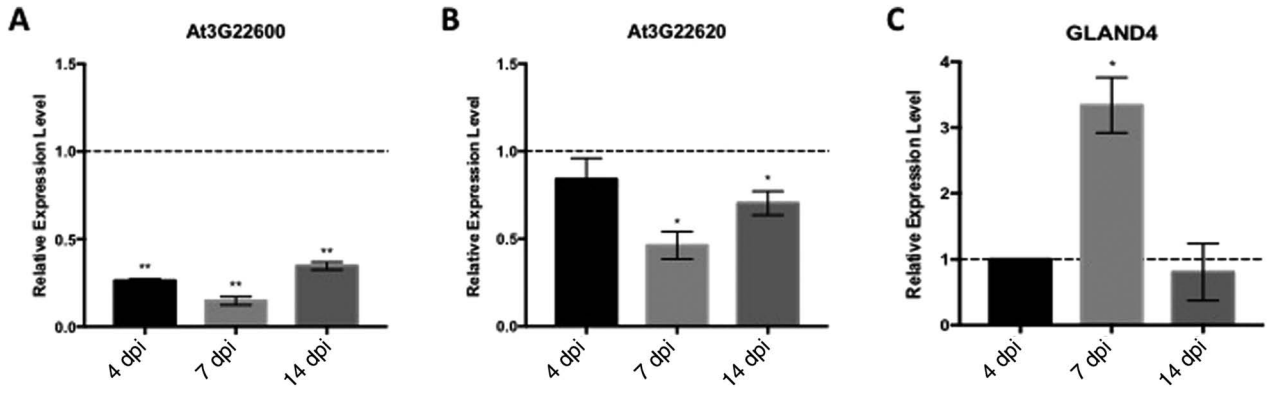

Fig. 6 Lipid transfer protein gene (*LTP*) down-regulation in wild-type roots is correlated with *GLAND4* expression levels. (A, B) Quantitative polymerase chain reaction (qPCR) was used to determine the *LTP* expression levels in the roots of *Heterodera schachtii*-infected and mock-treated wild-type Col-0 *Arabidopsis thaliana* at 4, 7 and 14 days post-inoculation (dpi). A *t*-test was used to compare the means between uninfected (set at 1.0), represented as a broken line, and infected roots at each time point. The data were normalized to *A. thaliana Actin8* as an internal control. (C) qPCR was used to determine *GLAND4* expression levels in the roots of H. schachtii-infected *A. thaliana* at 4, 7 and 14 dpi. A *t*-test was used to compare the means between 4 dpi (set at 1.0), represented as a broken line, and infected roots at subsequent time points. The data were normalized to *H. schachtii Actin* (AY443352). All results consist of two independent experiments, three biological replicates and four technical replicates. Bars represent the averages ± standard error (SE); $*P < 0.01$ and $**P < 0.0001$.

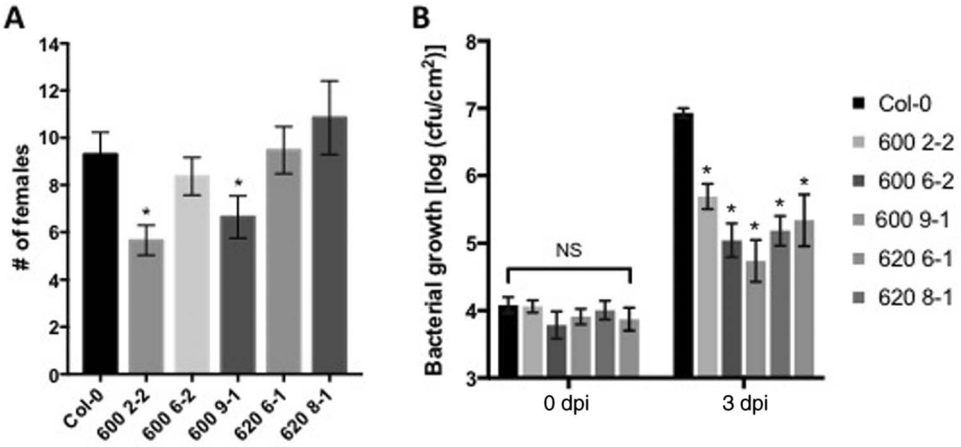

Fig. 7 Lipid transfer protein gene (*LTP*) overexpression reduces pathogen susceptibility. Independent homozygous *Arabidopsis thaliana* T3 lines overexpressing either *AT3G22600* (600 2-2, 600 6-2 and 600 9-1) or *AT3G22620* (620 6-1 and 620 8-1) were tested for alterations in susceptibility by counting the number of female nematodes present at 4 weeks post-inoculation with infective second-stage juveniles (A) or bacterial titres (cfu, colony-forming units) of leaves at 2h [0 days post-inoculation (dpi)] and 72h (3 dpi) after syringe infiltration with *Pseudomonas syringae* pv. *tomato* (*Pst* DC3000) (B). In (A), the bars represent the averages ± standard error (SE) and the data consist of two independent experiments, each with 20 plants. In (B), the bars represent the log transformed average ± SE from one of two independent experiments, each with four biological and three technical replicates. In both experiments, a *t*-test was used to determine differences in transgenic susceptibility relative to Col-0 *A. thaliana*. *$P < 0.05$; NS, not significant.

the *H. glycines* and *H. schachtii GLAND4* sequences highlighted GLAND4 as a strong candidate for characterization using the *H. schachtii–A. thaliana* model system. The generation of transgenic *A. thaliana* expressing a particular cyst nematode effector has proven to be useful in understanding the effector's role during the infection process. In some cases, ectopic expression of an effector results in an increased susceptibility to multiple pathogens, including *H. schachtii*, bacteria or an RNA virus, as well as alterations in defence marker gene expression (Hewezi *et al*., 2010, 2015; Lee *et al*., 2011). In this study, however, no change in susceptibility to *H. schachtii* was observed in transgenic plants expressing *GLAND4*. When considering that the function of GLAND4 is to repress genes that play a role in plant defences, this result is not unforeseeable, as *H. schachtii* is likely to already be secreting adequate amounts of GLAND4 required for successful infection. Transgenic plants producing high levels of GLAND4 showed an increased susceptibility to *P. syringae*, highlighting the impact of GLAND4 expression on plant defences in the absence of *H. schachtii*-derived GLAND4.

GLAND4 is one of many pioneer effectors produced by cyst nematodes that lack significant global alignment to known proteins, and, as such, protein structure and function prediction tools cannot provide reliable insights into the function of GLAND4 (Gao *et al*., 2001, 2003, Noon *et al*., 2015; Wang *et al*., 2001). Local alignment of GLAND4 to a histone-like repeat region alongside the confirmation of nuclear localization, performed as part of this study, provided a reason to test the hypothesis that GLAND4 functions as a DNA-binding protein. Genomic SELEX was used to investigate the potential DNA-binding properties of GLAND4, as this methodology has proven to be successful for a number of DNA-binding proteins (Chen *et al*., 2011; Shostak *et al*., 2004; Whittle *et al*., 2009). The resulting sequences were initially analysed for conserved elements that may allow for recognition by GLAND4, but this approach was unsuccessful. It is possible that the long input sequences caused background noise, thereby lowering the chance of finding small conserved motifs. Another possibility is that GLAND4 binds to a number of diverse sequences within the genome. One advantage of using genomic DNA instead of random short nucleotides is that the resulting sequences can be viewed in the context of their position within the organism's genome. Subsequent analyses focused on three *A. thaliana* genomic regions, two of which were located close to a TSS and one that was within the coding sequence for a member of the GRF family, which has been implicated previously in nematode infection (Hewezi *et al*., 2012). The selection of fragments located close to the TSS was, in part, based on the discovery that the plant-pathogenic bacteria *Xanthomonas* spp. secrete TALEs, which are known to bind to the promoter region of genes to activate host transcription (Kay *et al*., 2007). Subsequent EMSAs were able to ascertain that GLAND4 is the first plant-parasitic nematode effector to display DNA-binding properties, as all three tested fragments demonstrated some degree of delayed migration. The quantification of the shifted DNA bands indicated that G4RE2 was bound with a greater affinity than the two other tested fragments. Further testing of the preferential binding of GLAND4 to G4RE2 through the use of a competitive EMSA and

a non-specific DNA fragment supported further investigation into the G4RE2 region.

The two genes closely associated with G4RE2in *A. thaliana*, *AT3G22600* and *AT3G22620*, belong to a multigene family of LTPs that are present within a large number of plant species (Liu *et al.*, 2015). LTPs have been reported to perform a wide variety of functions, the most relevant of which include defence against biotic and abiotic stressors as well as systemic resistance signalling (Ambrose *et al.*, 2013; Jung *et al.*, 2003; Maldonado *et al.*, 2002; Sohal *et al.*, 1999). Analysis of *LTP* promoter regions from oilseed rape, rice and pepper showed an increase in activity after viral, fungal and bacterial attack, respectively (Guiderdoni *et al.*, 2002; Jung *et al.*, 2005; Sohal *et al.*, 1999). The induction of multiple *LTP*s, including *AT3G22600* and *AT3G22620*, has been observed in response to wounding or pathogen attack (Consales *et al.*, 2012; Larroque *et al.*, 2013; Molina and Garcia-Olmedo, 1993; Qutob *et al.*, 2006). AT3G22600 appears to be involved in pathogen-associated molecular pattern-triggered immunity, because this gene is highly up-regulated in response to *Phytophthora parasitica* cellulose-binding elicitor protein and oomycete-derived Nep1-like proteins (Larroque *et al.*, 2013; Qutob *et al.*, 2006). In the current study, *AT3G22600* and *AT3G22620* were both down-regulated in *GLAND4*-expressing *A. thaliana*, when compared with wild-type Col-0. The same two *LTP*s, which are already known to be down-regulated within the syncytia, were also found to be down-regulated in Col-0 root tissue during the course of cyst nematode infection, verifying that the down-regulation of *AT3G22600* and *AT3G22620* is a bona fide occurrence during *H. schachtii* infection (Szakasits *et al.*, 2009). Furthermore, a correlation in *GLAND4* expression and the expression of *AT3G22600* and *At3G22620* was also observed in the Col-0 time-course material, as *GLAND4* expression within the infecting nematodes peaked when *LTP* expression was at its lowest. Down-regulation of *AT3G22620* has been documented previously in response to oral secretions from the herbivorous insects *Pieris brassicae* and *Spodoptera littoralis* (Consales *et al.*, 2012). Collectively, these results, when considered alongside the repression of a reporter gene *in planta*, suggest that GLAND4 functions in the down-regulation of genes. Down-regulation of genes in the presence of GLAND4 is surprising given the similarity between the C-terminus of GLAND4 and characterized transcriptional activation domains. It is possible that the similarity to activator domains is required for GLAND4 to directly contact core machinery as part of a repression mechanism, which has been documented in rare instances (Payankaulam *et al.*, 2010).

To ascertain the importance of *LTP* down-regulation during *H. schachtii* infection, the *LTP* genes in question were individually overexpressed in *A. thaliana*. Elevated *AT3G22600* expression reduced *H. schachtii* susceptibility in two lines that expressed the coding sequence at a higher level (around 35-fold higher) than Col-0. Overexpression of *AT3G22620* did not alter *H. schachtii* susceptibility, indicating that the down-regulation of *AT3G22620* could be a by-product of targeting of *AT3G22600*. The hypothesis that *AT3G22600* is the primary target is also supported by previous findings which showed that *AT3G22600* is among the top 25 most down-regulated genes within the *H. schachtii* feeding site (Szakasits *et al.*, 2009). It is also possible that the AT3G22620 defence mechanism deployed against *H. schachtii* is limited by its dependence on a cofactor that was not increased in these transgenic lines. All transgenic lines for both LTPs displayed an enhanced resistance to *Pst* DC3000, which supports previous findings that the overexpression of a pepper *LTP* (*CALTP1*) in *A. thaliana* enhanced resistance to *Pst* DC3000 (Jung *et al.*, 2005).

This study characterizes GLAND4 as the first plant-parasitic nematode effector to bind to DNA, a finding which, until now, has only been eluded to on the basis of the discovery of a subset of effectors that share protein identity with histone and helicase DNA-binding regions (Bellafiore *et al.*, 2008; Gao *et al.*, 2003; Noon *et al.*, 2015). These findings provide the basis for future studies aimed at confirming the *in vivo* targets and regulation of host genes by GLAND4 and other newly discovered DNA-binding effectors.

EXPERIMENTAL PROCEDURES

In situ hybridization

Primers designed to the coding sequence of *HsGLAND4* were used to generate a 200-bp amplicon (Table S3, see Supporting Information). The resulting fragment was used as a template for unidirectional PCR to produce sense or antisense digoxigenin (DIG)-labelled DNA probes (Roche Life Sciences, Indianapolis, IN, USA). The probes were incubated with fixed, permeabilized mixed stage nematodes (de Boer *et al.*, 1998; Gao *et al.*, 2001). Probe detection was performed using alkaline phosphatase-conjugated anti-DIG antibody and substrate. A Zeiss (San Diego, CA, USA) Axiovert 100 inverted light microscope was used to visualize the specimens (de Boer *et al.*, 1998; Gao *et al.*, 2001). The results are a reflection of consistent findings in three independent hybridizations.

Subcellular localization

HsGLAND4^{-SP} was amplified using the sequence-specific primers HsG4_bait_F and HgG4_N1_R, and *HgGLAND4*$^{-SP}$ was amplified using HgG4_N1_F and HgG4_N1_R (Table S3). The PCR products were ligated into the *Bam*HI and *Eco*RI sites of pSAT6-EYFP-N1 (Tzfira *et al.*, 2005) at the N-terminus of YFP under the control of the CaMV 35S promoter (35S::*HsGLAND4*$^{-SP}$-YFP). The constructs were confirmed using Sanger sequencing. Transient expression was performed using ballistic bombardment

of onion epidermal cells (Bio-Rad, Hercules, CA, USA), as described previously (Elling *et al.*, 2007). YFP fluorescence was observed using a Zeiss Axiovert 100 inverted light microscope after the cells had been incubated in the dark at 26°C for 24h. This process was repeated for three independent experiments.

Genomic SELEX

FLAG-HsGLAND4^{-SP} was inserted into pET28a C-terminal His tag vector (Novagen, Madison, WI, USA) and expressed in Rosetta *E. coli* cells (Novagen). Cells were sonicated after induction with 0.2mM isopropyl-β-D-thiogalactoside for 2.5h at 37°C and FLAG-HsGLAND4^{-SP}-HIS was purified using nickel nitrilotriacetic acid agarose (Thermo Scientific, Waltham, MA, USA). Genomic SELEX was performed as published previously (Shostak *et al.*, 2004). Briefly, 5 μg of Sau3AI (Thermo Fisher Scientific, Waltham, MA, USA)-digested *A. thaliana* genomic DNA was incubated with 2 μg of purified recombinant FLAG-HsGLAND4^{-SP} -HIS tagged protein. The protein was immobilized using 30 μL of anti-FLAG affinity matrix (Sigma, St. Louis, MO, USA). After a series of wash steps, the DNA was eluted using binding buffer [20mM 4-(2-Hydroxyethyl)piperazine-1-ethanesulfonic acid at pH 7.9, 8% glycerol, 10mM $MgCl_2$, 10 μM $Zn(C_2H_3O_2)_2$] containing 1 M KCl. The eluted DNA was purified using Qiaquick columns (Qiagen, Valencia, CA, USA); adaptors were ligated for PCR. The DNA was subjected to three subsequent rounds of selection. After the final three rounds, an aliquot of the eluted DNA was ligated into the *Not*I site of pBluescriptIIKS+ (Stratagene, San Diego, CA, USA), transformed into DH5alpha. Sequences were obtained using Sanger sequencing.

EMSA

Double-stranded DNA fragments were amplified using sequence-specific primers (Table S3) and Col-0 genomic DNA as a template. The fragments were denatured, labelled with biotin using the Pierce Biotin End DNA Labeling Kit (Thermo Fisher Scientific) and reannealed. EMSAs were conducted using a LightShift Chemiluminescent EMSA Kit (Thermo Fisher Scientific). Nineteen picomoles of HsGLAND4^{-SP}-*HIS* or *Hs28B03*$^{-SP}$-*HIS* recombinant protein were incubated at room temperature for 20 min with 20 fmol biotin end-labelled, double-stranded oligonucleotides, 1 × binding buffer, 5mM $MgCl_2$, 0.05% (w/v) nonyl phenoxypolyethoxylethanol (NP-40) and 50 ng/μL (dI-dC) non-specific DNA competitor. In competitor reactions, 4, 6, 8 or 10 pmol of unlabelled oligonucleotides were included. Electrophoresis was performed using 6% Novex TBE 1.0-mm DNA retardation gels for 90 min at 100 V employing pre-chilled Novex 0.5 ×TBE running buffer (Thermo Fisher Scientific). The gel was transferred to a positively charged nylon membrane (PerkinElmer, Waltham, MA, USA). Biotin-labelled DNA was detected by immersing the membrane in streptavidin–horseradish peroxidase conjugate and chemiluminescent substrate (Thermo Fisher Scientific), followed by exposure to X-ray film (Research Products International, Mt Prospect, IL, USA). The quantification of DNA–protein complexes was measured as the ratio of intensity of the shifted band over the total amount loaded, as determined using ImageJ Software [National Institutes of Health (NIH), Bethesda, MD, USA].

Real-time qRT-PCR

Total RNA was isolated using a miCURY RNA Isolation Kit (Exiqon, Vedbaek, Denmark) according to the manufacturer's instructions. The RNA quantity and quality were assessed on a Thermo Scientific Nanodrop 2000. One microgram of total RNA was treated with DNase I (Thermo Fisher Scientific) and cDNA was synthesized using qScript cDNA SuperMix (Quantabio, Beverly, MA, USA). Two-step qRT-PCR was performed on an iCycler iQ Real-Time PCR machine with reactions containing 12.5 ng of template DNA, 300 nM of primers and the appropriate amount of iQ SYBR Green Supermix (Bio-Rad). The following thermocycler program was used: 95°C for 3 min, 40 cycles of 95°C for 15s and 60°C for 30s, followed by the establishment of a dissociation curve using the following program: 95°C for 1 min, 55°C for 10s and a slow ramp from 55 to 95°C. *Arabidopsis thaliana* and *H. schachtii* tissue were normalized using *Actin* as a reference gene (GenBank AY063089.1 and AY443352.1, respectively) (Table S3). Each qRT-PCR used three biological replicates and four technical replicates. The expression levels were calculated using the $2^{-\Delta\Delta CT}$ method (Livak and Schmittgen, 2001) and statistical differences were determined using a *t*-test in GraphPad Prism 4.

Generation of transgenic Arabidopsis

A FLAG tag was added to the N-terminus of *HsGLAND4*$^{-SP}$. Fragments for genomic insertion were amplified by PCR using gene-specific forward and reverse primers for *HsGLAND4*$^{-SP}$, AT3G22600 and AT3G22620 (Table S3). The digested fragments were ligated into the binary vector pBI121 and the sequence was confirmed using Sanger sequencing. The construct was transformed into *Agrobacterium tumefaciens* strain C58 using the freeze–thaw method. *Agrobacterium tumefaciens* was transformed into *A. thaliana* using the floral dip method, as described previously (Clough and Bent, 1998). The seeds were screened on Murashige and Skoog (MS) medium in the presence of 50mg/L kanamycin to select for transformants. Segregation analysis was conducted on T3 seeds to identify stable transgenic lines before their use in subsequent assays.

Nematode infection

Arabidopsis thaliana plants were surface sterilized and plated onto modified Knop's medium. After 10 days, 250 surface-sterilized J2 *H. schachtii* were inoculated onto the roots of each plant, as described previously (Baum *et al.*, 2000). Roots for the

time-course material were collected in liquid nitrogen after 4, 7 and 14 dpi from both inoculated and non-inoculated tissue. Seeds for the infection assays were plated into 12-well Falcon tissue culture plates (BD Biosciences, San Jose, CA, USA) in a randomized fashion. Females were counted after 3 weeks. Statistically significant differences between wild-type (Col-0) and transgenic lines were determined using a GraphPad Prism 4 *t*-test on 20 biological replicates and two independent experiments.

Bacterial growth assays

Pseudomonas syringae pv. *tomato* (*Pst* DC3000) was grown overnight in LB Rifampicin 50 mg/ml at 30°C and 250rpm. The bacteria were adjusted to 1.67×10^5 colony-forming units (cfu)/mL and syringe infiltrated into fully expanded 4–5-week-old leaves. Leaf discs were harvested, ground and plated onto LB Rif 50 at 2 and 72h post-inoculation. Graphs represent the log-transformed data from one of two independent experiments, each comprising four biological and three technical replicates. *t*-tests were performed using GraphPad Prism 4 to analyse the differences between wild-type (Col-0) and transgenic lines at each time point.

Plant transcriptional assays

To confirm the transcriptional repression of HsGLAND4^{-SP} in plant cells, the yeast Gal4BD–Upstream Activating Sequence system and the bacterial LexA–LexAop binding sequence were transferred into individual binary T-vectors, as shown previously (Tiwari *et al*., 2004; Zhang *et al*., 2015). Vector modifications and cloning information are listed in Methods S1 (see Supporting Information). Plasmids were then inserted into separate *A. tumefaciens* cells, strain GV3101, using the freeze–thaw method. A colony from each construct was grown overnight, and the cells were pelleted and resuspended in sterilized infiltration medium at a final optical density at 600nm (OD_{600}) of 0.4. The three sets of cells, the reporter and the two regulators, were combined in equal parts into one culture and syringe infiltrated into the entire leaf of three individual 6–8-week-old *Nicotiana benthamiana* plants. The leaves were ground in liquid nitrogen after 48h. RNA extraction, cDNA and qRT-PCR were performed as stated above. Infiltrated *N. benthamiana* tissue was measured for GFP expression and normalized using hygromycin as a reference gene (GenBank: FJ905225), as it is driven by CaMV 35S in all modified constructs (Table S3). The results are representative of three independent experiments conducted and analysed using GraphPad Prism 4.

ACKNOWLEDGEMENTS

This is a journal paper from the Iowa Agriculture and Home Economics Experiment Station, Ames, IA, USA, supported by Hatch Act and State of Iowa funds. This work was supported by funds from the Iowa Soybean Association. We thank T. R. Maier for technical assistance. The authors have no conflicts of interest to declare.

REFERENCES

Allen, T.W., Bradley, C.A., Sisson, A.J., Byamukama, E., Chilvers, M.I., Coker, C.M., Collins, A.A., Damicone, J.P., Dorrance, A.E., Dufault, N.S., Esker, P.D., Faske, T.R., Giesler, L.J., Grybauskas, A.P., Hershman, D.E., Hollier, C.A., Isakeit, T., Jardine, D.J., Kelly, H.M., Kemerait, R.C., Kleczewski, N.M., Koenning, S.R., Kurle, J.E., Malvick, D.K., Markell, S.G., Mehl, H.L., Mueller, D.S., Mueller, J.D., Mulrooney, R.P., Nelson, B.D., Newman, M.A., Osborne, L., Overstreet, C., Padgett, G.B., Phipps, P.M., Price, P.P., Sikora, E.J., Smith, D.L., Spurlock, T.N., Tande, C.A., Tenuta, A.U., Wise, K.A. and Wrather, J.A. (2017) Soybean yield loss estimates due to diseases in the United States and Ontario, Canada, from 2010 to 2014. *Plant Health Prog.* **18,** 19–27.

Ambrose, C., DeBono, A. and Wasteneys, G. (2013) Cell geometry guides the dynamic targeting of apoplastic GPI-linked lipid transfer protein to cell wall elements and cell borders in *Arabidopsis thaliana*. *PLoS One.* **8,** e81215.

Baum, T.J., Wubben, M.J.E., Hardy, K.A., Su, H. and Rodermel, S.R. (2000) A screen for *Arabidopsis thaliana* mutants with altered susceptibility to *Het erodera schachtii*. *J. Nematol.* **32,** 166–173.

Bellafiore, S., Shen, Z., Rosso, M.-N., Abad, P., Shih, P. and Briggs, S.P. (2008) Direct identification of the *Meloidogyne incognita* secretome reveals proteins with host cell reprogramming potential. *PLoS Pathog.* **4,** e1000192.

Bing, Y. and White, F.F. (2004) Diverse members of the AvrBs3/PthA family of type III effectors are major virulence determinants in bacterial blight disease of rice. *Mol. Plant–Microbe Interact.* **17,** 1192–1200.

de Boer, J.M., Yan, Y., Smant, G., Davis, E.L. and Baum, T.J. (1998) In-situ hybridization to messenger RNA in *Het erodera glycines*. *J. Nematol.* **30,** 309–312.

Chen, L.S., Zheng, J.S., Yang, N., Li, H. and Guo, S. (2011) Genomic selection identifies vertebrate transcription factor Fezf2 binding sites and target genes. *J. Biol. Chem.* **286,** 18 641–18 649.

Clough, S.J. and Bent, A.F. (1998) Floral dip: a simplified method for Agrobacterium-mediated transformation of *Arabidopsis thaliana*. *Plant J.* **16,** 735–743.

Consales, F., Schweizer, F., Erb, M., Gouhier-Darimont, C., Bodenhausen, N., Bruessow, F., Sobhy, I. and Reymond, P. (2012) Insect oral secretions suppress wound-induced responses in *Arabidopsis*. *J. Exp. Bot.* **63,** 727–737.

Cress, A. Triezenberg, S.J. (1991) Nucleotide and deduced amino-acid-sequences of the gene encoding virion protein-16 of herpes-simplex virus type-2. *Gene,* **103,** 235–238.

Elling, A.A., Davis, E.L., Hussey, R.S. and Baum, T.J. (2007) Active uptake of cyst nematode parasitism proteins into the plant cell nucleus. *Int. J. Parasitol.* **37,** 1269–1279.

Endo, B.Y. (1964) Penetration and development of *Het erodera glycines* in soybean roots and related anatomical changes. *Phytopathology,* **54,** 79.

Gao, B.L., Allen, R., Maier, T., Davis, E.L., Baum, T.J. and Hussey, R.S. (2001) Identification of putative parasitism genes expressed in the esophageal gland cells of the soybean cyst nematode *Het erodera glycines*. *Mol. Plant–Microbe Interact.* **14,** 1247–1254.

Gao, B.L., Allen, R., Maier, T., Davis, E.L., Baum, T.J. and Hussey, R.S. (2003) The parasitome of the phytonematode *Het erodera glycines*. *Mol. Plant–Microbe Interact.* **16,** 720–726.

Gheysen, G. and Fenoll, C. (2011) Arabidopsis as a tool for the study of plant–nematode interactions. In: Genomics and Molecular Genetics of Plant–Nematode Interactions (Jones, J.T., Gheysen, G., and Fenoll, C., eds.), pp. 139–156. Berlin: Springer-Verlag.

Guiderdoni, E., Cordero, M.J., Vignols, F., Garcia-Garrido, J.M., Lescot, M., Tharreau, D., Meynard, D., Ferrière, N., Notteghem, J.-L. and Delseny, M. (2002) Inducibility by pathogen attack and developmental regulation of the rice Ltp1 gene. *Plant Mol. Biol.* **49,** 683–699.

Hamamouch, N., Li, C., Hewezi, T., Baum, T.J., Mitchum, M.G., Hussey, R.S., Vodkin, L.O. and Davis, E.L. (2012) The interaction of the novel 30C02 cyst nematode effector protein with a plant beta-1,3-endoglucanase may suppress host defence to promote parasitism. *J. Exp. Bot.* **63,** 3683–3695.

Hermsmeier, D., Mazarei, M. and Baum, T.J. (1998) Differential display analysis of the early compatible interaction between soybean and the soybean cyst nematode. *Mol. Plant–Microbe Interact.* **11,** 1258–1263.

Hewezi, T. and Baum, T.J. (2013) Manipulation of plant cells by cyst and root-knot nematode effectors. *Mol. Plant–Microbe Interact.* **26,** 9–16.

Hewezi, T., Howe, P., Maier, T.R., Hussey, R.S., Mitchum, M.G., Davis, E.L. and Baum, T.J. (2008) Cellulose binding protein from the parasitic nematode *Het erodera schachtii* interacts with *Arabidopsis* pectin methylesterase: cooperative cell wall modification during parasitism. *Plant Cell*, **20,** 3080–3093.

Hewezi, T., Howe, P.J., Maier, T.R., Hussey, R.S., Mitchum, M.G., Davis, E.L. and Baum, T.J. (2010) *Arabidopsis* spermidine synthase is targeted by an effector protein of the cyst nematode *Het erodera schachtii*. *Plant Physiol.* **152,** 968–984.

Hewezi, T., Maier, T.R., Nettleton, D. and Baum, T.J. (2012) The *Arabidopsis* microRNA396-GRF1/GRF3 regulatory module acts as a developmental regulator in the reprogramming of root cells during cyst nematode infection. *Plant Physiol.* **159,** 321–335.

Hewezi, T., Juvale, P.S., Piya, S., Maier, T.R., Rambani, A., Rice, J.H., Mitchum, M.G., Davis, E.L., Hussey, R.S. and Baum, T.J. (2015) The cyst nematode effector protein 10A07 targets and recruits host posttranslational machinery to mediate its nuclear trafficking and to promote parasitism in *Arabidopsis*. *Plant Cell*, **27,** 891–907.

Hofmann, J., El Ashry, A., Anwar, S., Erban, A., Kopka, J. and Grundler, F. (2010) Metabolic profiling reveals local and systemic responses of host plants to nematode parasitism. *Plant J.* **62,** 1058–1071.

Hogenhout, S.A., Van der Hoorn, R.A.L., Terauchi, R. and Kamoun, S. (2009) Emerging concepts in effector biology of plant-associated organisms. *Mol. Plant–Microbe Interact.* **22,** 115–122.

Hussey, R.S. (1989) Disease inducing secretions of plant-parasitic nematodes. *Annu. Rev. Phytopathol.* **27,** 123–141.

Ithal, N., Recknor, J., Nettleton, D., Maier, T., Baum, T.J. and Mitchum, M.G. (2007) Developmental transcript profiling of cyst nematode feeding cells in soybean roots. *Mol. Plant–Microbe Interact.* **20,** 510–525.

Jaouannet, M., Perfus-Barbeoch, L., Deleury, E., Magliano, M., Engler, G., Vieira, P., Danchin, E.G.J., Da Rocha, M., Coquillard, P., Abad, P. and Rosso, M.-N. (2012) A root-knot nematode-secreted protein is injected into giant cells and targeted to the nuclei. *New Phytol.* **194,** 924–931.

Jones, J.T., Kumar, A., Pylypenko, L.A., Thirugnanasambandam, A., Castelli, L., Chapman, S., Cock, P.J., Grenier, E., Lilley, C.J., Phillips, M.S. and Blok, V.C. (2009) Identification and functional characterization of effectors in expressed sequence tags from various life cycle stages of the potato cyst nematode *Globodera pallida*. *Mol. Plant Pathol.* **10,** 815–828.

Jones, M.G.K. (1981) Host-cell responses to endo-parasitic nematode attack – structure and function of giant-cells and syncytia. *Ann. Appl. Biol.* **97,** 353.

Jones, M.G.K. and Northcote, D.H. (1972) Nematode-induced syncytium – multinucleate transfer cell. *J. Cell Sci.* **10,** 789.

Jung, H.W., Kim, W. and Hwang, B.K. (2003) Three pathogen-inducible genes encoding lipid transfer protein from pepper are differentially activated by pathogens, abiotic, and environmental stresses. *Plant Cell Environ.* **26,** 915–928.

Jung, H.W., Kim, K.D. and Hwang, B.K. (2005) Identification of pathogen-responsive regions in the promoter of a pepper lipid transfer protein gene (CALTPI) and the enhanced resistance of the CALTPI transgenic *Arabidopsis* against pathogen and environmental stresses. *Planta*, **221,** 361–373.

Kay, S., Hahn, S., Marois, E., Hause, G. and Bonas, U. (2007) A bacterial effector acts as a plant transcription factor and induces a cell size regulator. *Science*, **318,** 648–651.

Kim, J.-G., Taylor, K.W., Hotson, A., Keegan, M., Schmelz, E.A. and Mudgett, M.B. (2008) XopD SUMO protease affects host transcription, promotes pathogen growth, and delays symptom development in *Xanthomonas*-infected tomato leaves. *Plant Cell*, **20,** 1915–1929.

Koenning, S.R. and Wrather, J.A. (2010) Suppression of soybean yield potential in the continental United States by plant diseases from 2006 to 2009. *Plant Health Prog.* doi:10.1094/PHP-2010-1122-2001-RS.

de Lange, O., Schreiber, T., Schandry, N., Radeck, J., Braun, K.H., Koszinowski, J., Heuer, H., Strauß, A. and Lahaye, T. (2013) Breaking the DNA-binding code of *Ralstonia solanacearum* TAL effectors provides new possibilities to generate plant resistance genes against bacterial wilt disease. *New Phytol.* **199,** 773–786.

Larroque, M., Belmas, E., Martinez, T., Vergnes, S., Ladouce, N., Lafitte, C., Gaulin, E. and Dumas, B. (2013) Pathogen-associated molecular pattern-triggered immunity and resistance to the root pathogen *Phytophthora parasitica* in *Arabidopsis*. *J. Exp. Bot.* **64,** 3615–3625.

Laughon, A., and Gesteland, R.F. (1984) Primary structure of the saccharomyces-cerevisiae gal4 gene. *Mol. Cell. Biol.* **4,** 260–267.

Lee, C., Chronis, D., Kenning, C., Peret, B., Hewezi, T., Davis, E.L., Baum, T.J., Hussey, R., Bennett, M. and Mitchum, M.G. (2011) The novel cyst nematode effector protein 19C07 interacts with the *Arabidopsis* auxin influx transporter LAX3 to control feeding site development. *Plant Physiol.* **155,** 866–880.

Li, L., Atef, A., Piatek, A., Ali, Z., Piatek, M., Aouida, M., Sharakuu, A., Mahjoub, A., Wang, G., Khan, S., Fedoroff, N.V., Zhu, J.-K. and Mahfouz, M.M. (2013) Characterization and DNA-binding specificities of *Ralstonia* TAL-like effectors. *Mol. Plant*, **6,** 1318–1330.

Liu, F., Zhang, X., Lu, C., Zeng, X., Li, Y., Fu, D. and Wu, G. (2015) Non-specific lipid transfer proteins in plants: presenting new advances and an integrated functional analysis. *J. Exp. Bot.* **66,** 5663–5681.

Livak, K.J. and Schmittgen, T.D. (2001) Analysis of relative gene expression data using real-time quantitative PCR and the 2(T)(-Delta Delta C) method. *Met hods*, **25,** 402–408.

Lohmer, S., Maddaloni, M., Motto, M., Difonzo, N., Hartings, H., Salamini, F. and Gesteland, R.F. (1991) The maize regulatory locus opaque-2 encodes a dna-binding protein which activates the transcription of the b-32 gene. *Embo J.* **10,** 617–624.

Lozano-Torres, J.L., Wilbers, R.H.P., Gawronski, P., Boshoven, J.C., Finkers-Tomczak, A., Cordewener, J.H.G., America, A.H., Overmars, H.A., Van't Klooster, J.W., Baranowski, L., Sobczak, M., Ilyas, M., van der Hoorn, R.A., Schots, A., de Wit, P.J., Bakker, J., Goverse, A. and Smant, G. (2012) Dual disease resistance mediated by the immune receptor Cf-2 in tomato requires a common virulence target of a fungus and a nematode. *Proc. Natl. Acad. Sci. USA*, **109,** 10 119–10 124.

Maldonado, A.M., Doerner, P., Dixon, R.A., Lamb, C.J. and Cameron, R.K. (2002) A putative lipid transfer protein involved in systemic resistance signalling in *Arabidopsis*. *Nature*, **419,** 399–403.

Mitchum, M.G., Hussey, R.S., Baum, T.J., Wang, X., Elling, A.A., Wubben, M. and Davis, E.L. (2013) Nematode effector proteins: an emerging paradigm of parasitism. *New Phytol.* **199,** 879–894.

Molina, A. and Garcia-Olmedo, F. (1993) Developmental and pathogen-induced expression of 3 barley genes encoding lipid transfer proteins. *Plant J.* **4,** 983–991.

Nissan, G., Manulis-Sasson, S., Weinthal, D., Mor, H., Sessa, G. and Barash, I. (2006) The type III effectors HsvG and HsvB of gall-forming *Pantoea agglomerans* determine host specificity and function as transcriptional activators. *Mol. Microbiol.* **61,** 1118–1131.

Noon, J.B., Hewezi, T., Maier, T.R., Simmons, C., Wei, J.-Z., Wu, G., Llaca, V., Deschamps, S., Davis, E.L., Mitchum, M.G., Hussey, R.S. and Baum, T.J. (2015) Eighteen new candidate effectors of the phytonematode *Het erodera glycines* produced specifically in the secretory esophageal gland cells during parasitism. *Phytopathology*, **105,** 1362–1372.

Noon, J.B., Qi, M., Sill, D.N., Muppirala, U., Eves-van den Akker, S., Maier, T.R., Dobbs, D., Mitchum, M.G., Hewezi, T. and Baum, T.J. (2016) A plasmodium-like virulence effector of the soybean cyst nematode suppresses plant innate immunity. *New Phytol.* **212,** 444–460.

Padavannil, A., Jobichen, C., Qinghua, Y., Seetharaman, J., Velazquez-Campoy, A., Yang, L., Pan, S.Q. and Sivaraman, J. (2014) Dimerization of VirD2 binding protein is essential for *Agrobacterium* induced tumor formation in plants. *PLoS Pathog.* **10,** e1003948.

Patel, N., Hamamouch, N., Li, C.Y., Hewezi, T., Hussey, R.S., Baum, T.J., Mitchum, M.G. and Davis, E. (2010) A nematode effector protein similar to annexins in host plants. *J. Exp. Bot.* **61,** 235–248.

Payankaulam, S., Li, L.M. and Arnosti, D.N. (2010) Transcriptional repression: conserved and evolved features. *Curr. Biol.* **20,** R764–R771.

Pogorelko, G., Juvale, P.S., Rutter, W.B., Hewezi, T., Hussey, R., Davis, E.L., Mitchum, M.G. and Baum, T.J. (2016) A cyst nematode effector binds to diverse plant proteins, increases nematode susceptibility and affects root morphology. *Mol. Plant Pathol.* **17,** 832–844.

Postma, W.J., Slootweg, E.J., Rehman, S., Finkers-Tomczak, A., Tytgat, T.O.G., van Gelderen, K., Lozano-Torres, J.L., Roosien, J., Pomp, R., van Schaik, C., Bakker, J., Goverse, A. and Smant, G. (2012) The effector SPRYSEC-19 of *Globodera rostochiensis* suppresses CC-NB-LRR-mediated disease resistance in plants. *Plant Physiol.* **160,** 944–954.

Puthoff, D.P., Nettleton, D., Rodermel, S.R. and Baum, T.J. (2003) Arabidopsis gene expression changes during cyst nematode parasitism revealed by statistical analyses of microarray expression profiles. *Plant J.* **33,** 911–921.

Qutob, D., Kemmerling, B., Brunner, F., Küfner, I., Engelhardt, S., Gust, A.A., Luberacki, B., Seitz, H.U., Stahl, D., Rauhut, T., Glawischnig, E., Schween, G., Lacombe, B., Watanabe, N., Lam, E., Schlichting, R., Scheel, D., Nau, K., Dodt, G., Hubert, D., Gijzen, M. and Nürnberger, T. (2006) Phytotoxicity and innate immune responses induced by Nep1-like proteins. *Plant Cell*, **18,** 3721–3744.

Shostak, Y., Van Gilst, M.R., Antebi, A. and Yamamoto, K.R. (2004) Identification of C-elegans DAF-12-binding sites, response elements, and target genes. *Genes Dev.* **18,** 2529–2544.

Sijmons, P.C., Grundler, F.M.W., Mende, N., Burrows, P.R. and Wyss, U. (1991) *Arabidopsis-thaliana* as a new model host for plant-parasitic nematodes. *Plant J.* **1,** 245–254.

Sohal, A.K., Pallas, J.A. and Jenkins, G.I. (1999) The promoter of a *Brassica napus* lipid transfer protein gene is active in a range of tissues and stimulated by light and viral infection in transgenic *Arabidopsis*. *Plant Mol. Biol.* **41,** 75–87.

Sugio, A., Yang, B., Zhu, T. and White, F.F. (2007) Two type III effector genes of *Xanthomonas oryzae* pv. *oryzae* control the induction of the host genes OsTFIIA gamma 1 and OsTFX1 during bacterial blight of rice. *Proc. Natl. Acad. Sci. USA*, **104,** 10 720–10 725.

Szakasits, D., Heinen, P., Wieczorek, K., Hofmann, J., Wagner, F., Kreil, D.P., Sykacek, P., Grundler, F.M.W. and Bohlmann, H. (2009) The transcriptome of syncytia induced by the cyst nematode *Het erodera schachtii* in *Arabidopsis* roots. *Plant J.* **57,** 771–784.

Szurek, B., Marois, E., Bonas, U. and Van den Ackerveken, G. (2001) Eukaryotic features of the *Xanthomonas* type III effector AvrBs3: protein domains involved in transcriptional activation and the interaction with nuclear import receptors from pepper. *Plant J.* **26,** 523–534.

Tiwari, S.B., Hagen, G. and Guilfoyle, T.J. (2004) Aux/IAA proteins contain a potent transcriptional repression domain. *Plant Cell*, **16,** 533–543.

Tzfira, T., Tian, G.-W., Lacroix, B.T., Vyas, S., Li, J., Leitner-Dagan, Y., Krichevsky, A., Taylor, T., Vainstein, A. and Citovsky, V. (2005) pSAT vectors: a modular series of plasmids for autofluorescent protein tagging and expression of multiple genes in plants. *Plant Mol. Biol.* **57,** 503–516.

Vanholme, B., Kast, P., Haegeman, A., Jacob, J., Grunewald, W. and Gheysen, G. (2009) Structural and functional investigation of a secreted chorismate mutase from the plant-parasitic nematode *Het erodera schachtii* in the context of related enzymes from diverse origins. *Mol. Plant Pathol.* **10,** 189–200.

Vieira, P., Danchin, E.G.J., Neveu, C., Crozat, C., Jaubert, S., Hussey, R.S., Engler, G., Abad, P., de Almeida-Engler, J., Castagnone-Sereno, P. and Rosso, M.-N. (2011) The plant apoplasm is an important recipient compartment for nematode secreted proteins. *J. Exp. Bot.* **62,** 1241–1253.

Wan, J., Vuong, T., Jiao, Y., Joshi, T., Zhang, H., Xu, D. and Nguyen, H.T. (2015) Whole-genome gene expression profiling revealed genes and pathways potentially involved in regulating interactions of soybean with cyst nematode (*Het erodera glycines* Ichinohe). *BMC Genomics*, **16,** 148.

Wang, J., Lee, C., Replogle, A., Joshi, S., Korkin, D., Hussey, R., Baum, T.J., Davis, E.L., Wang, X. and Mitchum, M.G. (2010) Dual roles for the variable domain in protein trafficking and host-specific recognition of *Het erodera glycines* CLE effector proteins. *New Phytol.* **187,** 1003–1017.

Wang, X., Meyers, D., Yan, Y., Baum, T., Smant, G., Hussey, R. and Davis, E. (1999) In planta localization of a beta-1,4-endoglucanase secreted by *Het erodera glycines*. *Mol. Plant–Microbe Interact.* **12,** 64–67.

Wang, X., Allen, R., Ding, X., Goellner, M., Maier, T., de Boer, J.M., Baum, T.J., Hussey, R.S. and Davis, E.L. (2001) Signal peptide-selection of cDNA cloned directly from the esophageal gland cells of the soybean cyst nematode *Het erodera glycines*. *Mol. Plant–Microbe Interact.* **14,** 536–544.

Wang, X., Mitchum, M.G., Gao, B., Li, C., Diab, H., Baum, T.J., Hussey, R.S. and Davis, E.L. (2005) A parasitism gene from a plant-parasitic nematode with function similar to CLAVATA3/ESR (CLE) of *Arabidopsis thaliana*. *Mol. Plant Pathol.* **6,** 187–191.

Whittle, C.M., Lazakovitch, E., Gronostajski, R.M. and Lieb, J.D. (2009) DNA-binding specificity and in vivo targets of *Caenorhabditis elegans* nuclear factor I. *Proc. Natl. Acad. Sci. USA*, **106,** 12 049–12 054.

Yang, B., Zhu, W.G., Johnson, L.B. and White, F.F. (2000) The virulence factor AvrXa7 of *Xanthomonas oryzae* pv, *oryzae* is a type III secretion pathway-dependent nuclear-localized double-stranded DNA-binding protein. *Proc. Natl. Acad. Sci. USA*. **97,** 9807–9812.

Zhang, L., Davies, L.J. and Elling, A.A. (2015) A *Meloidogyne incognita* effector is imported into the nucleus and exhibits transcriptional activation activity in planta. *Mol. Plant Pathol.* **16,** 48–60.

Zhu, W.G., Yang, B., Chittoor, J.M., Johnson, L.B. and White, F.F. (1998) AvrXa10 contains an acidic transcriptional activation domain in the functionally conserved C terminus. *Mol. Plant. Microbe. In.* **11,** 824–832.

SUPPORTING INFORMATION

Additional supporting information may be found in the online version of this article at the publisher's web site:

Fig. S1 Pairwise sequence alignment of *GLAND4* from *Het erodera glycines* and *Het erodera schachtii*. Expasy translate was used to predict the protein sequence of polymerase chain reaction (PCR)-amplified fragments for the *H. glycines* and *H. schachtii GLAND4* orthologues. The sequences were aligned using EMBOSS needle with default settings to show 95% identity between the sequences. '|', matching amino acids, ':', similar conservative amino acids (share the same physicochemical properties); '.', non-conservative amino acids. The underline denotes the predicted N-terminal signal peptide (SignalP). The positively and negatively charged amino acids are marked with '+' and '*', respectively. Amino acids involved in the three overlapping bipartite nuclear localization signal predictions are marked with 'ν'.

Fig. S2 *GLAND4* expression in transgenic *Arabidopsis thaliana*. *GLAND4*$^{-SP}$ expression was measured in 3-week-old independent homozygous *A. thaliana* T3 lines (3-10, 5-6 and 6-1) using quantitative polymerase chain reaction (qPCR). Data were normalized to *Actin* as an internal control. The means and standard error (SE) are reflective of two independent experiments, each with three biological replicates and four technical replicates. A *t*-test was used to determine the fold difference relative to the mean of the lowest expressing line, 3-10 (set at 1.0), marked as a broken line. The bars represent the averages ± SE. $^*P < 0.01$.

Fig. S3 Nematode susceptibility in *GLAND4*-transgenic *Arabidopsis thaliana*. The numbers of female nematodes were counted on independent homozygous *A. thaliana* T3 lines (3-10, 5-6 and 6-1) constitutively expressing *GLAND4*$^{-SP}$ at 4 weeks post-inoculation with infective second-stage juveniles. Data were collected from two independent experiments, each with 20 plants. The bars represent the averages ± standard error (SE). A one-way analysis of variance (ANOVA) was performed to determine no statistical difference between the Col-0 mean and *GLAND4*$^{-SP}$-expressing plants.

Fig. S4 *AT3G22600* and *AT3G22620* expression in transgenic *Arabidopsis thaliana*. (A) *AT3G22600*. (B) *AT3G22620*. Gene expression was measured in independent homozygous *A. thaliana* T3 lines overexpressing either *AT3G22600* (600 2-2, 600 6-2 and 600 9-1) or *AT3G22620* (620 6-1 and 620 8-1) using quantitative polymerase chain reaction (qPCR). Data were normalized to *A. thaliana Actin8* as an internal control. The means and ± standard error (SE) are reflective of two independent experiments, each with three biological replicates and four technical replicates. A *t*-test was used to determine the fold difference relative to Col-0, marked as a broken line (set at 1.0). $^*P < 0.01$.

Table S1 Comparison of the C-terminus of GLAND4 with characterized activation domains from: AvrXa10 (Zhu *et al.*, 1998), OPAQUE-2 (Lohmer *et al.*, 1991), VP16 (Cress and Triezenberg, 2015) and GAL4 (Laughon and Gesteland, 1984). Acidic residues are shown in bold. Bulky or hydrophobic residues are underlined.

Table S2 A BLASTP search was performed against the non-redundant protein database using the repeat region from GLAND4. Provided in the table are GenBank accession numbers, descriptions and alignment lengths with percentage identities to hits with known or predicted histone-related functions.

Table S3 Primer list.

Methods S1 Plant transcriptional assays—vector modifications and cloning information.